

Study of the PWM Control Strategies for Three Switches Isolated Boost DC-DC Converter

Truong-Duy Duong¹, Minh-Khai Nguyen², Young-Cheol Lim¹ and Joon-Ho Choi¹

¹ Department of Electrical Engineering, Chonnam National University, Gwangju 500-757, Korea.

² Department of Electrical Engineering, Chosun University, Gwangju 61452, Korea.
E-mail: nmkhai00@gmail.com

Abstract. This paper presents the PWM control strategies for three-switch isolated boost DC-DC converter. By inserting the extra states into the conduction time of switches, the current input is still continuous; unchanged primary and secondary voltage waveforms of the high-frequency (HF) transformer. The parameter design guideline with the different PWM control strategies is discussed. A 400 W prototype has been tested in the laboratory to verify the performance of the three-switch DC-DC converter with two PWM control strategies and a PI controller was used to clarify the DC output voltage at 400 V. The simulation and experimental results are shown to validate the theoretical analysis.

1. Introduction

In recent year, the development of further industrial technology and the enormous consumption of electrical energy lead to exhaust the natural resources, many environmental problems occur. So, the development clean energy are the most-effective solution, such as wind, solar, and fuel cells... The distributed generation technologies is used to generate the energy sources which have a low-voltage DC and instability. In order to connect them to the residential loads, the power-conversion system is widely used, as shown in Figure 1. In the DC-DC converter stage, a high step-up DC-DC converter is utilized to convert the low voltage of the renewable sources into 200V or 400V DC voltage [1], [2]. In the second-stage, the DC-AC inverter is used to provide the AC voltage 110 V_{rms} or 220 V_{rms} to connect grid for the industrial application.

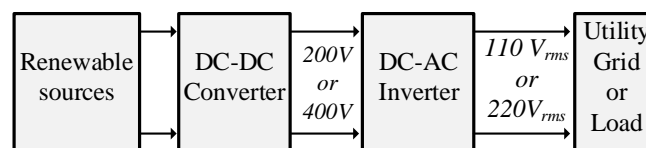


Figure 1. Typical power-conversion system.

High step-up DC-DC converters have been proposed and consider to obtain a high-voltage gain, such as isolated and non-isolated topologies. For non-isolated topologies, many researchers have proposed a lot of converter, it consists of a cascade topology [3], couple inductor [4], a switched-capacitor, a switched-inductor [5], [6] and the mixture of them [7], [8]. The non-isolated topologies are without HF transformer, so the system volume and cost is cheap. However, to have the isolation between input and output source, achieve the high voltage step-up gain, many isolated topologies have been presented in [9]-[11]. For isolated topologies, the voltage-fed and current-fed topologies are widely used. The



voltage gain of the voltage-fed DC-DC converters [11], [12] is provided mainly by a HF transformer. In order to achieve a high gain, the turn ratio of the transformer must be large. Nevertheless, the current-fed converter have a boost ability by using the boost inductor connect directly to the input voltage, and it is suitable for applications with high step-up ratio. Hence, the input current ripple and turn ratio of the HF transformer in current-fed topologies is lower than those in voltage-fed topologies in [13]-[15].

Compared to the conventional current-fed full-bridge (CFFB) DC-DC converter in [16], [17], the three-switch isolated boost DC-DC converter has some advantages, which are as follows: 1) the input current is continuous with low ripple; 2) it uses one fewer active switch and 3) the snubber circuit is not used. In this paper, the PWM control strategies for three-switch isolated boost DC-DC converter are proposed in this paper. To verify the analysis, simulation and experimental results are provided.

2. Proposed PWM control strategies for three-switch DC-DC converter

The three-switch isolated DC-DC converter, as shown in Figure 2, it's consists of a boost inductor (L_1), three switches, one boost capacitor (C_1), one diode (D_1) in the primary winding of the transformer, voltage doubler rectifier (VDR) circuit include two diodes (D_2 and D_3) and two output capacitors (C_2 and C_3), and resistor load (R).

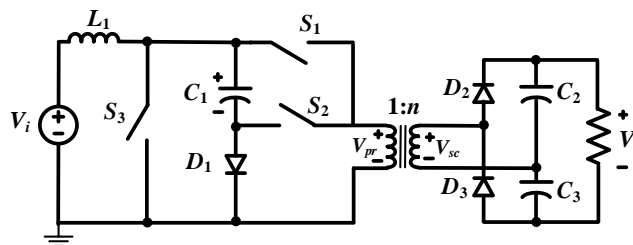


Figure 2. The three-switch isolated boost DC-DC converter.

2.1. PWM Control Strategies

The pulse-width-modulation (PWM) control methods for the three-switch DC-DC converter are shown in Figure 3. In Figure 3(a), the PWM control method 1, the extra states are inserted into gate signal of switches S_1 and S_3 to extend the ON time interval of two switches S_1 and S_3 . The extra states are inserted into the zero state of the period, thus the positive and negative of the primary voltage is only kept at $0.3T$. We can change the gain voltage by changing the ON time interval of the switches, the primary and secondary voltage waveforms is unchanged.

Similarly, the PWM control method 2 is shown in Figure 3(b), the extra states is also inserted into the zero state of the period. So, the primary and voltage waveforms is similar the PWM control method 1.

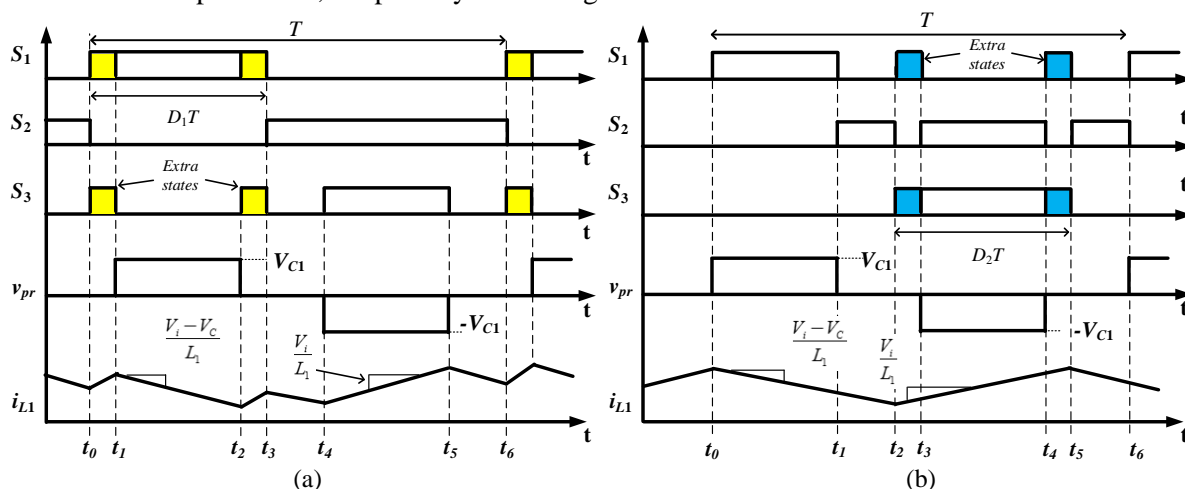


Figure 3. PWM control strategies. (a) PWM method 1 and (b) PWM method 2.

2.2. Operating principle of the three-switch DC-DC converter with PWM control method 1

For the operation analysis of circuit, the performed conditions are following as: 1) operate in continuous conduction mode (CCM); 2) all devices are ideal; 3) the high-frequency transformer is modeling by an ideal transformer; 5) the capacitance of the capacitors is sufficient to keep a constant capacitor voltage; the AC pulse primary and secondary voltage waveforms of the HF transformer is 30% positive, 20% zero, 30% negative, and 20% zero sequentially, respectively.

Stage 1— $[t_0 - t_1, t_2 - t_3]$, Figure 4(a): At t_0 , the extra state is inserted into the on time interval of S_1 and S_3 . Furthermore, S_1, S_3 are turned on and S_2 is turned off. The inductor L_1 is charged by the input voltage.

$$L_1 \frac{di_{L1}}{dt} = V_i, \quad (1)$$

Stage 2— $[t_1 - t_2]$, Figure 4(b): S_1 is turned on, S_2 and S_3 are turned off. The inductor L_1 is discharge. The primary voltage of the transformer is V_{C1} . We have:

$$L_1 \frac{di_{L1}}{dt} = V_i - V_{C1}, \quad (2)$$

Stage 3— $[t_3 - t_4, t_5 - t_6]$, Figure 4(c): In this time, only S_2 is turned on. The diode D_1 is forward-bias and the inductor L_1 current is through diode D_1 . The primary voltage of the transformer is shorted by diode D_1 . Thus, the secondary voltage of the transformer is zero; the D_2 and D_3 diodes are reverse-biased. We get:

$$L_1 \frac{di_{L1}}{dt} = V_i - V_{C1}, \quad (3)$$

Stage 4— $[t_4 - t_5]$, Figure 4(d): At t_4 , S_3 and S_2 is turned on, S_1 remains off. The inductor L_1 is charged, when the capacitor C_1 is discharged. The primary voltage of the transformer is $-V_{C1}$. Hence, the secondary voltage is negative in which passed through the step-up transformer. The voltage of the inductor L_1 is calculated as

$$L_1 \frac{di_{L1}}{dt} = V_i, \quad (4)$$

By using the volt-second balance law to the inductor L_1 , from (1)-(4), the capacitor C_1 voltage and output voltage gain can be determined as

$$\begin{cases} V_{C1} = \frac{1}{1-D_1} V_i \\ G = \frac{V_o}{V_i} = \frac{2n}{1-D_1} \end{cases}, \quad (5)$$

Where D_1 is the time on of switch S_1 in the PWM method 1.

The operating principle for PWM method 2 is analyzed similarly with the PWM method 1. And we get the capacitor C_1 voltage (V_{C11}) and output voltage gain (G_1), respectively, can be calculated as

$$\begin{cases} V_{C11} = \frac{1}{1-D_2} V_i \\ G_1 = \frac{V_o}{V_i} = \frac{2n}{1-D_2} \end{cases}, \quad (6)$$

Where D_2 is the time on of switch S_1 in the PWM method 2.

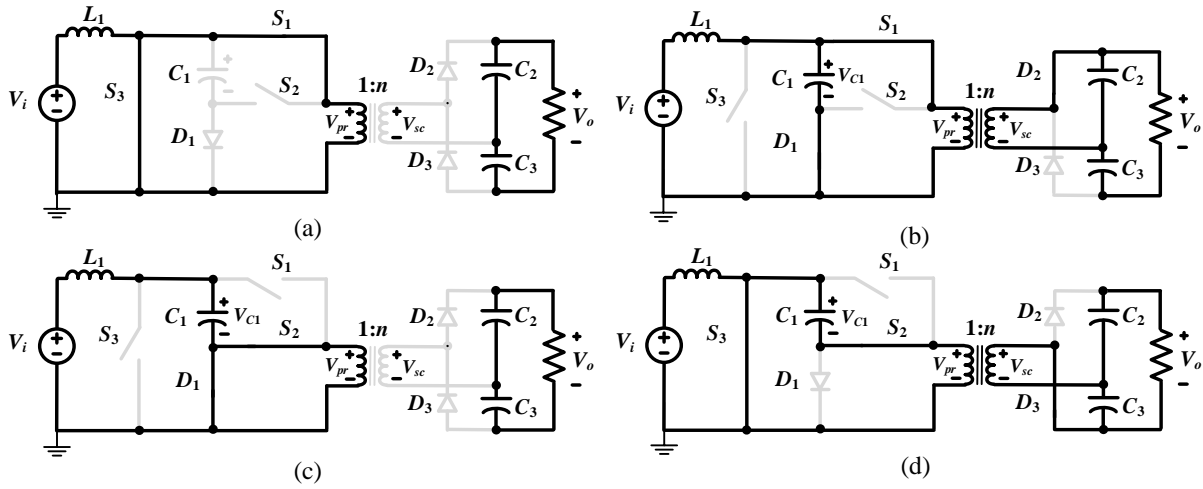


Figure 4. Key waveforms of the three-switch converter with PWM control method 1.

2.3. The PI control algorithms for the three-switch converter

The PI controller is used to keep the output voltage is constant at 400 V, and the diagram is shown in Figure 5. The error signal between the output voltage and the reference voltage of 400 V is through the PI controller. The PI control output is determined by the limiter module. The PWM generator is generated by the PWM control method 1 or method 2, and the gate signals of the S_1 , S_2 and S_3 switches is created from the PWM generator.

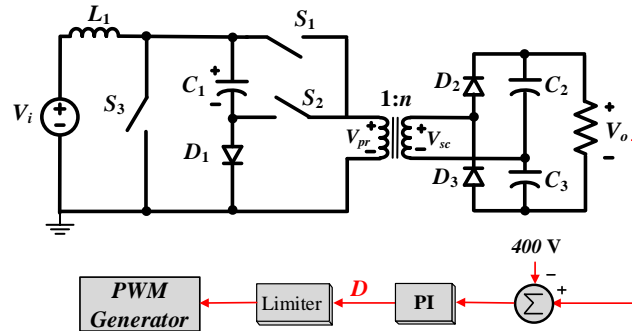


Figure 5. PI control diagram for the three-switch DC-DC converter.

3. Parameters Selection

3.1. Inductance Selection

Based on the PWM control method 1 is shown as in Figure 3(a). When the secondary voltage is negative, the peak-to-peak inductor L_1 current with $D_1 < 0.5$ is determined as

$$\Delta I_{L1} = \frac{0.3V_i}{f \cdot L_1}, \quad (7)$$

Where f is the switching frequency.

When $D_1 \geq 0.5$, the peak-to-peak inductor L_1 current is calculated

$$\Delta I_{L1} = \frac{0.3D_1V_g}{(1-D_1)fL_1}. \quad (8)$$

The inductor current ripple of the three-switch converter for PWM method 1 is calculated as

$$\Delta I_{L1} = r_{L1} \% \cdot I_{L1}, \quad (9)$$

The L_1 inductance is defined in

$$L_1 = \begin{cases} \frac{0.3V_i^2}{r_{L1}\% fP_o}, & D_1 < 0.5 \\ \frac{0.3D_1V_i^2}{(1-D_1)r_{L1}\% fP_o}, & D_1 \geq 0.5. \end{cases} \quad (10)$$

For the PWM control method 2 is shown as in **Figure 3(b)**. The peak-to-peak inductor L_1 current is calculated as

$$\Delta I_{L1} = \frac{D_2 V_i}{f \cdot L_1}, \quad (11)$$

The L_1 inductance in this case is determined as

$$L_1 = \frac{D_2 V_i^2}{r_{L1}\% fP_o}, \quad (12)$$

3.2. Capacitance Selection

Both the PWM control method 1 and the PWM control method 2, the negative state of the primary voltage waveform is $0.3T$. Thus, the capacitor C_1 is designed base on the current flow to it. We have the current C_1 is

$$C_1 \frac{\Delta V_{C1}}{0.3T} = |n \bar{i}_{sc}|. \quad (13)$$

The capacitor C_1 is defined as

$$C_1 = \frac{0.3(1-D)^2 P_o}{r_{C1}\% fV_{dc}^2}. \quad (14)$$

Where $r_{C1}\%$ is the capacitor voltage ripple.

The capacitor C_2 and C_3 of the VDR module can be selected in the zero mode time. If the ripple voltage of the C_2 and C_3 capacitors is $r_c\%$.

$$\begin{cases} C_2 = C_3 = \frac{0.4(1-D_1)^2 P_o}{4f \cdot r_c\% n^2 V_i^2}, & \text{for PWM method 1} \\ C_2 = C_3 = \frac{0.4(1-D_2)^2 P_o}{4f \cdot r_c\% n^2 V_i^2}, & \text{for PWM method 2.} \end{cases} \quad (15)$$

4. Simulation and Experimental Results

4.1. Simulation Results

The three-switch DC-DC converter with two method PWM control is verified by using PSIM 9.1 simulation. The frequency of switching is 10 kHz. The simulation parameters is chosen from Table 1. These simulation results are agreeable with the theoretical analysis. In Figures 6-7, the output voltage of 400 V is boosted from the input voltage of 40 V with two methods PWM control. The input current is continuous with two PWM methods. The primary and secondary voltage waveforms of the transformer are not changed, when the PWM methods are applied.

Table 1. Parameters for simulation and experiment.

Parameter	Value
Output voltage	400 V
Output power	400 W
Input voltage	40 V
Inductors (L_1)	1 mH
HF transformer	1:2.5
Capacitors C_1	330 uF
$C_2 = C_3$	82 uF
Switching frequency	10KHz

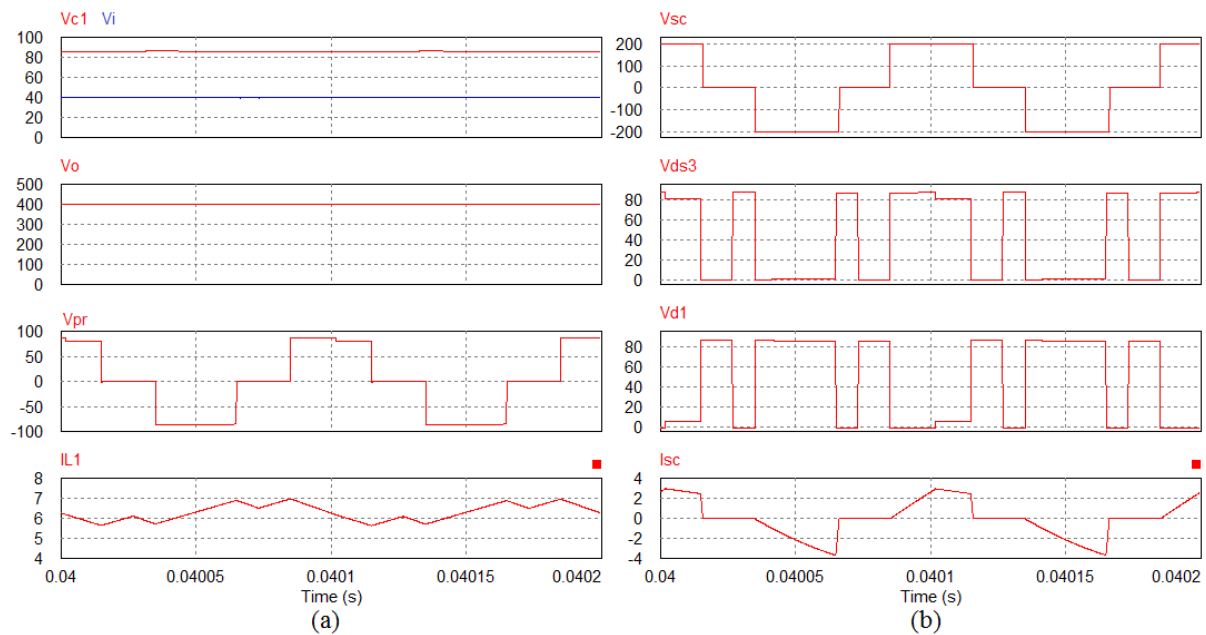


Figure 6. Simulation results with PWM method 1 when $V_i = 40$ V.

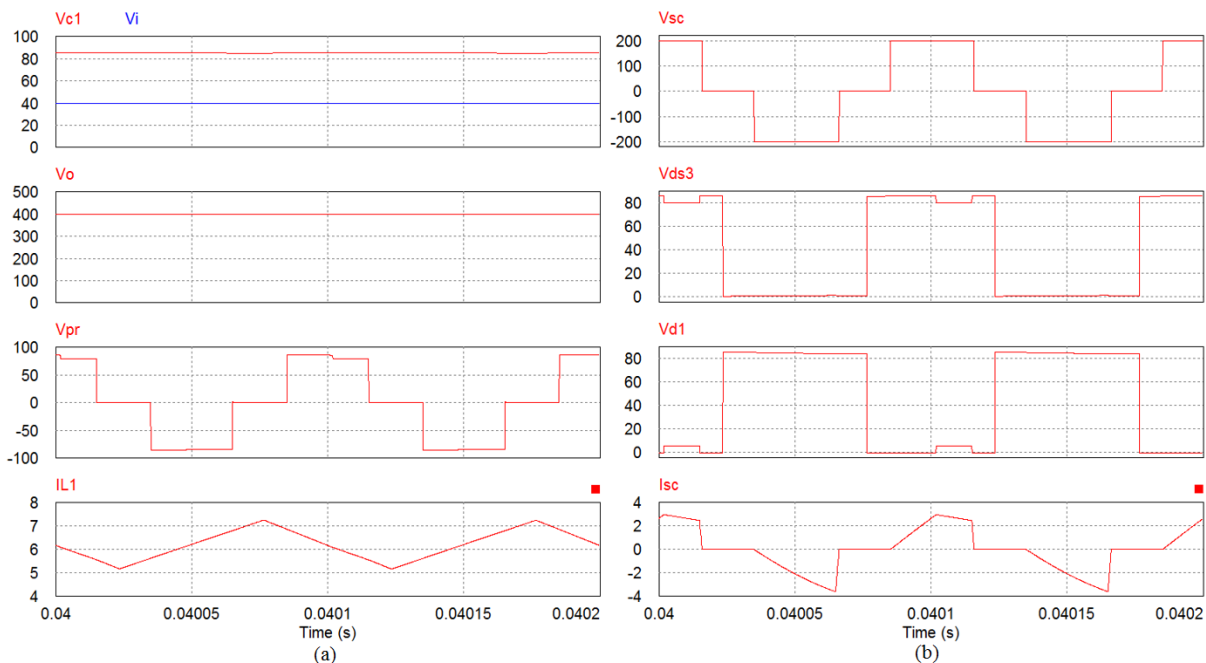


Figure 7. Simulation results with PWM method 2 when $V_i = 40$ V.

4.2. Experimental Results

In order to demonstrate the PWM control strategies are proposed in Section II, the experiment results with 400 W are implemented by using DSP kit TMS320F28335. The parameters experiments are used, as shown in Table 1.

One boost inductor is 1 mH/ 20 A is used to connect to the input voltage by direction, one boost capacitor is 330 μ F/ 200 V. Two 82 μ F/ 450 V capacitors were used for the secondary side of the HF transformer. The switches and diodes are IRFP460 MOSFETs and DSEP30-12A diodes. The PWM signals are generated by TMS320F28335 through the isolated amplifiers (TLP250) and the gating signal to drive all MOSFETs.

Figure 8 shows the experimental results for the PWM control method 2 when the input voltage and the power load are 40 V and 260 W, respectively. An extra states are inserted into the PWM signals

generation like to the PWM method 1 and method 2. The voltage C_1 voltage was 85 V for the PWM control method 1 and 86 V for the PWM control method 2. The input current of two PWM control method are continuous. But the peak-to-peak ripple inductor L_1 current for PWM method 1 is lower than that the peak-to-peak ripple inductor L_1 current for PWM method 2. These simulation and experimental results are suitable for the theoretical analysis.

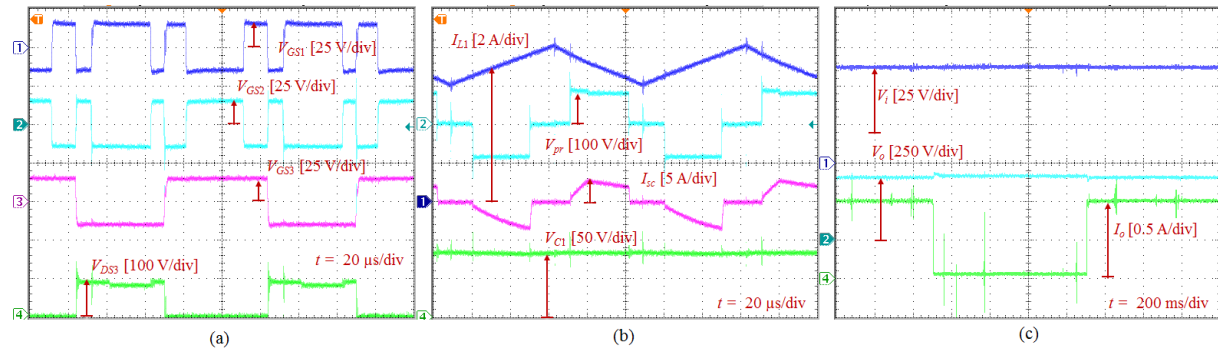


Figure 8. Experimental results with PWM method 2 when $V_i = 40$ V.

In Figure 8, the key waveforms are the gating signals of MOSFETs S_1 - S_3 voltage, drain-source MOSFETs S_3 voltage; the inductor L_1 current, primary voltage, the secondary current, and load current. The transient response of PI controller of the three-switch DC-DC converter is shown in Fig. 8(c), the waveforms from top to bottom are the input voltage, the load voltage, and the load current, respectively. In this case, the input voltage is generated at 40 V when the step change of power load occur from full load (400 W) to light load (21 W). The stable operation in case that the graph has a very small obvious overshoot.

5. Conclusion

PWM control strategies for three-switch isolated boost DC-DC converter has been presented in this paper and had the following characteristics: the current input is continuous with two PWM strategies; unchanged primary and secondary voltage waveforms of the HF transformer. The inductance and capacitance selection of the circuit are shown. The operating principles and analysis of converter are depicted with PI controller. The proposed converter is applicable for fuel-cell applications with low-dc input voltage.

6. References

- [1] S. M. Chen, T. J. Liang, L. S. Yang, and J. F. Chen, "A boost converter with capacitor multiplier and coupled inductor for ac module applications," *IEEE Trans. Ind. Electron.*, vol. 60, no. 4, pp. 1503–1511, April 2013.
- [2] G. Wu, X. Ruan, and Z. Ye, "Nonisolated high step-up DC-DC converters adopting switched-capacitor cell," *IEEE Trans. Ind. Electron.*, vol. 62, no. 1, pp. 383–393, January 2015.
- [3] Y. J. A. Alcazar, D. S. Oliveira, Jr., F.L. Tofoli, and R.P. Torrico-Bascopé, "DC-DC Nonisolated boost converter based on the three-state switching cell and voltage multiplier cells," *IEEE Trans. Ind. Electron.*, vol. 60, no. 10, pp. 4438–4449, Oct. 2013. Y. P. Hsieh, J. F. Chen, T. J. Liang, and L. S. Yang, "Novel high step-up DC-DC converter with coupled-inductor and switched-capacitor techniques," *IEEE Trans. Ind. Electron.*, vol. 59, no. 2, pp. 998–1007, Feb. 2012.
- [4] A. I. Bratcu, I. Munteanu, S. Bacha, D. Picault, and B. Raison, "Cascaded DC-DC converter photovoltaic systems: power optimization issues," *IEEE Trans. Ind. Electron.*, vol. 58, no. 2, pp. 403–411, February 2011.

- [5] L. S. Yang and T. J. Liang, "Analysis and implementation of a novel bidirectional DC-DC converter," *IEEE Trans. Ind. Electron.*, vol. 59, no. 1, pp. 422–434, Jan. 2012.
- [6] B. Axelrod, Y. Beck, and Y. Berkovich, "High step-up dc-dc converter based on the switched-coupled-inductor boost converter and diode-capacitor multiplier: steady state and dynamics," *IET Power Electron.*, vol. 8, no. 8, pp. 1420–1428, 2015.
- [7] R. Y. Chen, T. J. Liang, J. F. Chen, R. L. Lin, and K. C. Tseng, "Study and implementation of a current-fed full-bridge boost dc-dc converter with zero-current switching for high-voltage applications," *IEEE Trans. Ind. Appl.*, vol. 44, no. 4, pp. 1218–1226, July/Aug. 2008.
- [8] M. Nymand, and M. A. E. Andersen, "High-efficiency isolated boost dc-dc converter for high-power low-voltage fuel-cell applications," *IEEE Trans. Ind. Electron.*, vol. 57, no. 2, pp. 505–514, Feb. 2010.
- [9] Z. Zhang, O. C. Thomsen and M. A. E. Andersen, "Soft-switched dual-input DC-DC converter combining a boost-half-bridge cell and a voltage-fed full-bridge cell" *IEEE Trans. Ind. Electron.*, vol. 28, no. 11, pp. 4897–4902, Feb. 2013.
- [10] C. Yao, X. Ruan, and X. Wang, "Automatic mode-shifting control strategy with input voltage feed-forward for full-bridge-boost dc-dc converter suitable for wide input voltage range," *IEEE Trans. Power Electron.*, vol. 30, no. 3, pp. 1668–1682, March 2015.
- [11] A. Mohammadpour, L. Parsa, M. H. Todorovic, R. Lai, R. Datta, and L. Garces, "Series-input parallel-output modular-phase dc-dc converter with soft-switching and high-frequency isolation," *IEEE Trans. Power Electron.*, vol. 31, no. 1, pp. 111–119, Jan. 2016.
- [12] Z. Zhang, O. C. Thomsen, M. A. E. Andersen, and H. R. Nielsen, "Dual-input isolated full-bridge boost dc-dc converter based on the distributed transformers," *IET Power Electron.*, vol. 5, no. 7, pp. 1074–1083, Aug. 2012.
- [13] U. R. Prasanna, and A. K. Rathore, "Extended Range ZVS Active-Clamped Current-Fed Full-Bridge Isolated DC/DC Converter for Fuel Cell Applications: Analysis, Design, and Experimental Results," *IEEE Trans. Ind. Electron.*, vol. 60, no. 7, pp. 2661–2672, July 2013.
- [14] M. Nymand, and M. A. E. Andersen, "High-efficiency isolated boost dc-dc converter for high-power low voltage fuel-cell applications," *IEEE Trans. Ind. Electron.*, vol. 57, no. 2, pp. 505–514, Feb. 2010.
- [15] M. K. Nguyen, L. C. Lim, J. H. Choi, and G. B. Cho "Isolated High Step-up DC-DC Converter Based on Quasi-Switched-Boost Network". *IEEE Trans. Ind. Electron.*, vol. 63, no. 12, pp. 7553–7562, Dec. 2016.
- [16] A. Mohammadpour, L. Parsa, M. H. Todorovic, R. Lai, R. Datta, and L. Garces, "Series-input parallel-output modular-phase dc-dc converter with soft-switching and high-frequency isolation," *IEEE Trans. Power Electron.*, vol. 31, no. 1, pp. 111–119, Jan. 2016.
- [17] Z. Zhang, O. C. Thomsen, M. A. E. Andersen, and H. R. Nielsen, "Dual-input isolated full-bridge boost dc-dc converter based on the distributed transformers," *IET Power Electron.*, vol. 5, no. 7, pp. 1074–1083, Aug. 2012.